



## Assessment of simvastatin niosomes for pediatric transdermal drug delivery

Ahmed S. Zidan, Khaled M. Hosny, Osama A. A. Ahmed & Usama A. Fahmy

To cite this article: Ahmed S. Zidan, Khaled M. Hosny, Osama A. A. Ahmed & Usama A. Fahmy (2016) Assessment of simvastatin niosomes for pediatric transdermal drug delivery, Drug Delivery, 23:5, 1536-1549, DOI: [10.3109/10717544.2014.980896](https://doi.org/10.3109/10717544.2014.980896)

To link to this article: <https://doi.org/10.3109/10717544.2014.980896>



Published online: 11 Nov 2014.



Submit your article to this journal [↗](#)



Article views: 2214



View related articles [↗](#)



View Crossmark data [↗](#)



Citing articles: 3 View citing articles [↗](#)

## RESEARCH ARTICLE

# Assessment of simvastatin niosomes for pediatric transdermal drug delivery

Ahmed S. Zidan<sup>1,2</sup>, Khaled M. Hosny<sup>1,3</sup>, Osama A. A. Ahmed<sup>1,4</sup>, and Usama A. Fahmy<sup>1</sup>

<sup>1</sup>Department of Pharmaceutics and Industrial Pharmacy, Faculty of Pharmacy, King Abdulaziz University, Jeddah, KSA, <sup>2</sup>Department of Pharmaceutics and Industrial Pharmacy, Faculty of Pharmacy, Zagazig University, Zagazig, Egypt, <sup>3</sup>Department of Pharmaceutics and Industrial Pharmacy, Faculty of Pharmacy, Beni Suef University, Beni Suef, Egypt, and <sup>4</sup>Department of Pharmaceutics and Industrial Pharmacy, Faculty of Pharmacy, Minia University, Minia, Egypt

## Abstract

The prevalence of childhood dyslipidemia increases and is considered as an important risk factor for the incidence of cardiovascular disease in the adulthood. To improve dosing accuracy and facilitate the determination of dosing regimens in function of the body weight, the proposed study aims at preparing transdermal niosomal gels of simvastatin as possible transdermal drug delivery system for pediatric applications. Twelve formulations were prepared to screen the influence of formulation and processing variables on critical niosomal characteristics. Nano-sized niosomes with 0.31  $\mu\text{m}$  number-weighted size displayed highest simvastatin release rate with 8.5% entrapment capacity. The niosomal surface coverage by negative charges was calculated according to Langmuir isotherm with  $n = 0.42$  to suggest that the surface association was site-independent, probably producing surface rearrangements. Hypolipidemic activities after transdermal administration of niosomal gels to rats showed significant reduction in cholesterol and triglyceride levels while increasing plasma high-density lipoproteins concentration. Bioavailability estimation in rats revealed an augmentation in simvastatin bioavailability by 3.35 and 2.9 folds from formulation F3 and F10, respectively, compared with oral drug suspension. Hence, this transdermal simvastatin niosomes not only exhibited remarkable potential to enhance its bioavailability and hypolipidemic activity but also considered a promising pediatric antihyperlipidemic formulation.

## Keywords

Bioavailability, hypolipidemic activity, niosomes, simvastatin, transdermal delivery system

## History

Received 9 October 2014  
Revised 22 October 2014  
Accepted 22 October 2014

## Introduction

Dyslipidemia is one of the most important risk factors for many chronic non-communicable diseases resulting in serious morbidity, and mortality, and medical costs worldwide (Smith, 2007). This situation has become apparent given the economic growth and associated sociodemographic, dietary and lifestyle changes in recent decades coupled with a reduced burden of infectious diseases (WHO-Report, 2012). There is strong evidence of development of atherosclerotic cardiovascular disease that begins early in life, even in childhood (Newman et al., 1986; Hakanen et al., 2006; Amati et al., 2007). The prevalence of fibrous plaques considerably increases from 8% to 69% from childhood to young adulthood (Hakanen et al., 2006). The rise in total cholesterol, low-density lipoprotein (LDL), cholesterol, triglycerides (TG), blood pressure, and body mass index and multiple risk factors can be correlated with the incidence of cardiovascular disease in childhood (Pesonen, 1989; Dahl-Jorgensen et al., 2005;

Schwab et al., 2007). This knowledge accompanied by a rise in obesity, type 2 diabetes and hypertension in older children and adults, caused the American Academy of Pediatrics to issue goals of “improving lipid and lipoprotein concentrations during childhood and adolescence to lower the lifelong risk of cardiovascular diseases (CVD)” (Daniels et al., 2008).

Statins are one of the most widely prescribed medications in the USA and have been shown to be effective at reducing coronary morbidity and mortality in high-risk adults (Belay et al., 2007). Depending on the patient baseline values and the dose used, these medications result in cholesterol reductions of 20–50% below baseline (Daniels et al., 2008). Due to their history of efficacy in adults, statins are one of the first-line medications considered for use in the pediatric population with dyslipidemia (Belay et al., 2007; Ceballos et al., 2008; Gelissen et al., 2014). Currently, only limited dosage forms of statins are available. All statins are available in tablet formulations (Tiwari & Pathak, 2011). Simvastatin is offered as a disintegrating oral tablet designed for adults; however, limited products are available for use in the pediatric population with improved patient compliance. Regardless of the documented short-term efficacy and safety of statins in children above 10 years old, significant issues remain with use in this patient population (Belay et al., 2007).

Address for correspondence: Ahmed S. Zidan, Department of Pharmaceutics and Industrial Pharmacy, Faculty of Pharmacy, King Abdulaziz University, P.O. Box: 80260, Jeddah 21589, KSA. Tel: (00966) 564 266 682. Fax: (00966) 126 951 696. E-mail: aszidan@kau.edu.sa; azidoon@yahoo.com

Different concerns existed such as possible negative effects on muscles, growth and/or maturation, and potential teratogenicity in a population that includes adolescent females (Sibley & Stone, 2006; Belay et al., 2007). Despite the fact that these are all theoretical concerns with scarce clinical evidences, long-term administration remained definitely an important risk (Browne & Vasquez, 2008).

Simvastatin exists as crystalline powder with a melting point of 135–138 °C and is practically insoluble in water and poorly absorbed from the gastro-intestinal tract (Kang et al., 2004). The first pass metabolism is also responsible for its poor oral bioavailability that approximated by 5% (Gambhire et al., 2011). Different approaches have been applied to improve the solubility of simvastatin, including nanocrystals, co-solvency, recrystallization and self-emulsification (Kang et al., 2004; Pandya et al., 2008; Varshosaz et al., 2011; Jiang et al., 2012; El-Say et al., 2014). However, none of these methods has been applied to propose simvastatin in a transdermal niosomal formulation for pediatric applications. Proposing simvastatin in transdermal preparation would offer more advantages over the oral administration including but not limited to avoiding first pass metabolism, achieving sustained release features, bypassing the complications of the gastrointestinal tract on drug absorption, reducing the dosage rate, hence improving patient tolerability (Ammar et al., 2008). Moreover, being a noninvasive administration route, discontinuation of drug action can be done easily by removal from skin surface (Ah et al., 2010; Bariya et al., 2012). It is our hypothesis that preparation of simvastatin in a systematically optimized transdermal niosomal formulation will not only increase its bioavailability and percutaneous absorption but also improve its efficacy for better control of the plasma lipid profile.

Niosomes can be formed by diluting its viscous liquid crystalline compacts with aqueous medium (El-Menshawe & Hussein, 2013). The processing steps for their manufacturing and subsequent dilution would affect their *in vitro* and *in vivo* performance. In addition, the modification of the lamellar integrity as well as their surface charge type and intensity would influence the release of the entrapped drug and their interaction with the target site (Tavano et al., 2011). In addition to the chemical stability of the employed amphiphiles, the liquid crystalline nature shows an enhanced physical and chemical stability such as their resistance to

aggregation, fusion and/or drug leakage upon storage. The easiness of manufacturing and low cost of starting materials makes niosomes an attractive approach for scale up processing (Zidan et al., 2011). In this regard, the present study reports preparation of simvastatin in a transdermal niosomal gels for improving its hypolipidemic efficacy. The study included the application of Plackett–Burman screening design to mine important processing and formulation parameters. The proposed formulations were characterized in terms of their vesicular size, surface morphology, drug leakage, surface charge intensity, and *in vivo* pharmacodynamic and pharmacokinetic performance in rats.

## Materials and methods

Simvastatin was supplied by Saudi Arabian Japanese Pharmaceutical Co. (SAJA) (Jeddah, Saudi Arabia). Sorbitan monolaurate and sorbitan monostearate (span 20 and 60, respectively) were purchased from Ruger Chemical Co., Inc. (Linden, NJ). Cholesterol, stearylamine and dicetyl phosphate were purchased from VWR International Co. (Bridgeport, NJ). Dibasic sodium phosphate and sodium dodecyl sulfate were purchased from Sigma-Aldrich Corporation (St. Louis, MO). Phosphate buffer solution (pH 6.8), HPLC grade acetonitrile and ethanol were purchased from Thermo Fisher Scientific Inc. (Pittsburgh, PA).

## Niosomes preparation

Simvastatin-loaded niosomes were prepared according to the reported method by Zidan et al. with some modifications (Zidan & Mokhtar, 2011). Twelve formulations were prepared using different combination and loadings of the employed excipients according to Plackett–Burman screening design (Table 1). In particular, the specified amounts of simvastatin, amphiphile (namely span 20 or 60), surface charge imparting agent (namely stearylamine or dicetyl phosphate) and cholesterol were transferred into a 30 mL scintillation vials and about 2 mL of ethanol was added to dissolve the lipids at 60 °C. Two milliliters of distilled water was then added to the organic phase while vortexing to form a viscous niosomal liquid crystalline phase. The organic solvent was subsequently evaporated using the rotary evaporator for 2 h followed by dilution with 30 mL distilled water to form niosomal suspensions. The obtained niosomal suspensions were then sonicated

Table 1. Composition and processing variables of different simvastatin-loaded niosomal formulations according to Plackett–Burman screening design.

Batch #	Surfactant loading (moles)		Cholesterol loading (moles)	Charging agent type	Charging agent loading (%)	Sonication time (seconds)	Sonication amplitude	Drug loading (moles)
	X1	X2						
F1	1	Span 20	0.2	Positive	5	30	40	0.3
F2	1	Span 20	0.6	Negative	5	90	20	0.9
F3	1	Span 20	0.6	Negative	10	90	40	0.3
F4	1	Span 60	0.2	Negative	10	30	40	0.9
F5	1	Span 60	0.2	Positive	10	90	20	0.3
F6	1	Span 60	0.6	Positive	5	30	20	0.9
F7	2	Span 20	0.2	Negative	10	30	20	0.9
F8	2	Span 20	0.2	Positive	5	90	40	0.9
F9	2	Span 20	0.6	Positive	10	30	20	0.3
F10	2	Span 60	0.2	Negative	5	90	20	0.3
F11	2	Span 60	0.6	Negative	5	30	40	0.3
F12	2	Span 60	0.6	Positive	10	90	40	0.9

according to the sonication parameters for each experiment for diminution of large vesicles (Table 1). Excess un-entrapped drug was removed by centrifugation (Eppendorf Centrifuge, Model 5415 C, Eppendorf-Netheler-Hinz GmbH 2000, Hamburg, Germany) at 35 000 rpm for 2 h. The resultant residue was reconstituted with 2 mL of pH 6.8 phosphate buffer for further analysis.

### Microscopic analysis

The surface features of simvastatin-loaded niosomes were investigated using an electronic transmission microscope (TEM) (JEM-100CX/II, JEOL Ltd., Tokyo, Japan). The niosomal suspension was adsorbed on a copper grid coated with carbon film followed by air drying and then staining with 2% phosphotungstic acid for image capturing. On the other hand, a scanning electron microscope (SSX-500, Shimadzu, Kyoto, Japan) was utilized at an accelerating voltage of 15 kV to capture SEM images of the niosomal formulation, after sputter coating with gold/palladium under vacuum.

### Drug entrapment capacity

After harvesting the niosomal vesicles by ultracentrifugation, the free drug was determined in the supernatant using an in-house developed and validated analytical chromatographic method. In particular, Hewlett-Packard (HP) HPLC instrument (Agilent Technologies, Palo Alto, CA) equipped with HP 1200 UV detector set at a wavelength of 238 nm, HP 1200 autosampler and a quaternary HP 1200 pump was used. The HP thermostatted column compartment was set at 32 °C. The chromatographic separation was accomplished by injecting 10 µL samples onto Luna(2) RP-18 (250 × 4.6 mm, 5 µm packing) reverse phase analytical column (Phenomenex, Torrance, CA). The mobile phase was composed of acetonitrile–phosphate buffer (pH 6.8; 0.01 M) (40:60, v/v) with an isocratic flow rate of 1.2 mL/minute. The detected number of moles of simvastatin loaded in niosomal vesicles was compared with the number of moles of lipids in each sample. The capacity of vesicles to entrap simvastatin was evaluated using the following equation of weight concentration ratio, where  $C_m$  is the number of moles of simvastatin entrapped within  $C_l$  moles of lipids:

$$EC = \frac{C_m}{C_l} \times 100$$

### Vesicular size analysis

The vesicular size of the niosomes was determined using a Zetasizer 3000 (Malvern Instruments, Worcestershire, UK) equipped with a goniometry, a uniphase 22 mV He–Ne laser operating at 632.8 nm and an avalanche photodiode and detector. Light scattering was monitored at 90°. After diluting 1 mL of the niosomal suspension with 300 mL of distilled water, the size data acquisition was performed at 25 °C.

### Surface charge analysis

The surface charge parameters, namely zeta potential, net charge, conductivity and electrophoretic mobility, of the niosomal systems were measured using the same instrument

used for vesicular size determination. The zeta potential was determined for each sample in 10 replicates.

### Drug release characteristics

A niosomal suspension equivalent to 1 mg/mL simvastatin was prepared in 10 mM phosphate buffer (pH 6.8), and 0.5 mL of it was inserted into the donor compartment of Franz diffusion cells (Hanson research, MicroettePlus, Chatsworth, CA). The diffusion apparatus was composed of 1.76 cm<sup>2</sup> of diffusion area, receptor chamber volume of 7 mL and cellulose ester dialysis membrane of 20 kDa molecular weight cut-off. The samples were dialyzed against 10 mM phosphate buffer (pH 6.8) containing 0.05% sodium dodecyl sulfate to maintain sink condition (acceptor) at 37 °C and stirring rate of 300 rpm. At specified time points (0.5–12 h), 0.2 mL aliquots were withdrawn from the acceptor media and analyzed for simvastatin leakage percentage by the developed chromatographic method. The experiment was repeated with 1 mg/mL simvastatin solution to determine its intrinsic diffusion across cellulose ester membrane (control).

### In vivo hypolipidemic activity

Animal study protocol was approved by the local Institutional Review Board for Preclinical and Clinical Research (Faculty of Pharmacy, King Abdulaziz University, Jeddah, KSA). The protocol was designed to ensure the care and use of animals complied with the Declaration of Helsinki and the Guiding Principle in Care and Use of Animals (DHEW publication NIH 80-23) and the ‘Principles of Laboratory Animal Care’ (NIH publication #85-23, revised in 1985). The hypolipidemic activity of the drug-loaded niosomal systems was evaluated in male Sprague-Dawley rats (200–300 g). The animals were divided into four groups (six rats each) and kept for seven days with free access to standard diet and water. Prior beginning the experiments, the animals were fasted overnight and blood samples were collected through retro-orbital puncturing to determine the baseline levels of serum cholesterol, TG and high-density lipoproteins (HDL). Comparing these biochemical parameters after administering the drug-loaded niosomes with the corresponding baseline values was done using paired *t*-test of significance so that each animal served as its own control. The four groups were nominated as a control group received plain distilled water, a positive control group received oral simvastatin suspension through esophageal intubation, and two test groups received simvastatin-loaded niosomal formulation number 3 and 10 (lowest and highest drug release rates, respectively). For inducing hypercholesterolemia in rats, TG-rich diet containing 25% soybean oil, 1.0% cholesterol, 13% fiber and 4538.4 kcal/kg was used. This diet promoted increment of LDL, TG, cholesterol with a reduction in the HDL fraction with minor effect on hepatic function of the animals (Matos et al., 2005). After three weeks, animals were administered the control and test formulations by oral gavage and transdermal application, respectively, for five days. For transdermal delivery, the hair at the back of the animals was trimmed. A square was drawn on the back of each rat and 100 µL of niosomal gel was applied. The blood samples were withdrawn after 5, 10 and 15 days of treatment. Serum was

separated and assayed for cholesterol, TG and HDL by *in vitro* diagnostic kits (Randox Laboratories Ltd., London, UK). The test of significance for the variation in the lipid profile among the control and treatment groups was done using paired *t*-test; where an obtained *p* values less than 0.05 were described significant. The protection percent calculated as decreasing cholesterol level by the drug-loaded niosomal formulation against the control was calculated using the following equation, where  $CH_{\text{control}}$  and  $CH_{\text{treated}}$  were the percent increment of cholesterol concentration in control and treatment groups, respectively:

$$\text{Protection percent} = \frac{CH_{\text{control}} - CH_{\text{treated}}}{CH_{\text{treated}}} \times 100$$

### Bioavailability studies

Bioavailability analysis was done in rats in an attempt to explore the capability of the transdermal niosomal formulations in improving simvastatin's pharmacokinetic parameters. Male Sprague-Dawley rats weighing ~300 g were used for the experiments. The rats were fasted for 12 h prior to administering the drug formulation with free access to water. The animals were divided into three groups to administer oral simvastatin suspension (group I, positive control), and two niosomal formulations with lowest and highest drug release rates (groups II and III to administer formulations F3 and F10, respectively). The drug suspension was administered by intraesophageal intubation at a dose of 20 mg/kg. After trimming the back hair at one square spot, the niosomal formulations were applied transdermally at a dose equivalent to 20 mg/kg. At predetermined time intervals, 0.5 mL of blood samples was withdrawn into heparinized tube by retro-orbital puncture. The blood samples were then centrifuged at 10 000g for 8 min to separate the plasma was followed by storing in sterile polypropylene vials at  $-20^{\circ}\text{C}$  until further chromatographic analysis. Quantitation of the drug in plasma samples was done using isocratic chromatographic elution equipped with an ultraviolet spectroscopic detector set at 235 nm. Chromatographic separation was performed on Luna(2) RP-18 ( $250 \times 4.6$  mm,  $5 \mu\text{m}$  packing) reverse phase analytical column (Phenomenex, Torrance, CA) at  $32^{\circ}\text{C}$ . The mobile phase was composed of acetonitrile:water:ortho phosphoric acid at 65:35:0.1% v/v (pH 2.8). The mobile phase was pumped isocratically at a flow rate of 1.25 mL/min. For simvastatin extraction from plasma samples, the protein was precipitated with 60% perchloric acid at a working volume ratio to plasma volume of 1:5 v/v. The resultant acidic solution was then vortexed for 10 min followed by centrifugation at 6000 rpm for 10 min. The internal standard ( $2 \mu\text{L}$  of 0.5 mg/mL carbamazepine solution in mobile phase) was added to 500  $\mu\text{L}$  of the separated supernatant followed by extracting with 5 mL diethyl ether and 1 mL potassium hydroxide solution (4M). After vortexing and centrifuging, the supernatants were evaporated under nitrogen and the residues were constituted with 200  $\mu\text{L}$  of mobile phase for injection. The developed bioanalytical chromatographic method was in-house validated and deemed precise, accurate, sensitive, selective and robust. The limits of quantitation and detections were 2 and 0.5 ng/mL, respectively.

### Results and discussion

Based on the Plackett–Burman design of experiments with a resolution of III, this study proposed a screening approach to formulate simvastatin in a niosomal transdermal formulation. This approach proposed formulation methods and compositions for treating pediatric patients in need of statin drug therapy, for example, for hyperlipidemia and hypercholesterolemia syndromes. The embodiments of this study were designed to potentiate the clinical efficacy of the drug while reducing or eliminating the side effects that commonly occur with statin drugs. Through the Plackett–Burman design, each independent factor was investigated in two levels, high and low. In the present study, the niosome manufacturing process was screened for eight variables at two levels (Table 1). The eight assigned variables were screened in 12 experimental designs in which each row represents an experiment and each column represents an independent variable. The characteristics of the prepared systems were grouped into four categories, namely vesicular size, electrical, entrapment and release parameters, and determined for each experiment (Table 2). Wide variations in the investigated responses were observed to reflect the importance of the screening study to mine the most important and significant variables.

#### Vesicular size

To explore how the formulation's chemical and physical variables would affect the vesicular size, the vesicular size was investigated using two size-weighing strategies, namely volume and number weighing. Volume-weighted vesicular size correlates to the mass distribution of the niosomal vesicles and the area under the curve of each size distribution peak denotes the relative percentage of that signal (Xu et al., 2012). Since the intensity of the scattered light by the Brownian movement of the vesicles is weighted by both the mass and the other vesicular factors, the hydrodynamic diameter can be influenced by the scattering angle (Patty & Frisken, 2006). This influence is remarkable for large and widely distributed vesicles. Therefore, the number-weighted vesicular size that does not affected by the scattering angle would be more preferred (Tables 2 and 3). The obtained size analysis data showed that the prepared niosomal sizes were smaller after sonication. However, a non-significant size reduction was observed for the recorded volume-weighted sized rather than number-weighted ones. For the various factors' combinations, Table 2 shows that the volume-weighted vesicular size ranged from 1.55  $\mu\text{m}$  (F4) to 4.09  $\mu\text{m}$  (F8). On the other hand, the number-weighted vesicular size ranged from 0.31  $\mu\text{m}$  (F10) to 4.21  $\mu\text{m}$  (F12). The most significant factors affecting both volume- and number-weighted vesicular size were incorporated percentage of charging agent and sonication time ( $p < 0.05$ ) (Table 3 and Figure 1). Amphiphile loading and type of charging agent (negative rather than positive charges) were only significant to the volume-weighted sizes. In addition, sonication amplitude and experimental simvastatin loading were only significant to number-weighted sizes. The ‘‘Estimate’’ column in Table 3 expresses each variable's relative strength to the other factors, the higher the absolute value the more the effect of that variable on the investigated response. In addition, a

Table 2. Characterization of the prepared simvastatin-loaded niosomal formulations.

Batch #	Vesicular size (volume weighted- $\mu\text{m}$ )	Vesicular size (number weighted- $\mu\text{m}$ )	Electrophoretic mobility ( $\mu\text{s/V/cm}$ )	Zeta potential (mV)	Surface charge (fC)	Conductivity ( $\mu\text{S/cm}$ )	Drug release parameters <sup>a</sup>			
							Polarity	EC (%)	Q 1 h (%)	Q 12 h (%)
F1	2.42	0.48	0.57	7.26	0.138	12	Negative	16.7	1.54	13.65
F2	2.46	2.09	1.31	16.77	0.333	19	Positive	37.4	0.15	1.36
F3	1.97	1.88	2.18	27.91	0.445	20	Negative	12.4	0.81	12.58
F4	1.55	2.68	2.14	27.44	0.28	16	Negative	44.9	17.09	63.15
F5	2.52	0.41	1.65	23.1	0.282	14.5	Positive	16.6	13.74	40.07
F6	2.90	0.84	0.5	6.36	0.02	12	Positive	37.4	4.01	21.92
F7	2.34	1.70	2.62	33.54	0.597	22	Negative	29.4	12.36	74.22
F8	4.09	2.90	0.65	8.37	0.338	17	Positive	27	11.84	72.66
F9	2.44	0.36	1.61	20.61	0.315	20	Negative	4.1	5.26	42.33
F10	3.16	0.31	3.57	42.55	0.997	12.3	Negative	8.5	32.57	89.77
F11	3.20	0.43	2.28	34.16	1.01	13.7	Positive	7.6	12.92	59.51
F12	3.68	4.21	1.74	22.3	0.547	20	Negative	23	12.81	73.78

<sup>a</sup>Q 1 h and Q 12 h are percentage of simvastatin released after 1 and 12 h, respectively.

Table 3. Results of multiple regression analysis for prediction of the investigated responses.

Factors	Vesicular size (volume weighted- $\mu\text{m}$ )	Vesicular size (number weighted- $\mu\text{m}$ )	Electrophoretic mobility ( $\mu\text{s/V/cm}$ )	Zeta potential (mV)	Surface charge (fC)	Conductivity ( $\mu\text{S/cm}$ )	EC (%)	Q 1 h (%) <sup>a</sup>	Q 12 h (%) <sup>a</sup>
Intercept									
Estimate	2.835	1.481	1.980	25.985	0.523	14.750	23.000	15.183	58.030
p value	<.0001	0.0019	0.0006	<.0001	0.0008	<.0001	<.0001	0.0017	0.0002
Surfactant loading (X1)									
Estimate	0.424	0.127	0.343	4.391	0.192	0.958	-5.483	-4.372	-21.630
p value	0.0084	0.2947	0.0343	0.0035	0.0054	0.0194	0.0022	0.0216	0.0016
Surfactant chain length (X2)									
Estimate	0.215	-0.089	0.490	6.908	0.162	3.583	1.833	-9.857	-21.897
p value	0.2133	0.6876	0.0778	0.0070	0.0554	0.0033	0.1991	0.0156	0.0111
Cholesterol loading (X3)									
Estimate	0.047	0.111	-0.132	-1.179	0.003	0.908	-1.767	4.262	11.838
p value	0.5400	0.3497	0.2513	0.1083	0.9124	0.0224	0.0489	0.0231	0.0090
Charging agent type (X4) (Negative)									
Estimate	-0.282	-0.009	0.615	7.864	0.169	0.625	1.283	2.062	3.017
p value	0.0257	0.9359	0.0070	0.0006	0.0079	0.0580	0.1051	0.1290	0.2193
Charging agent loading (X5)									
Estimate	-0.311	-0.349	0.255	3.286	-0.031	2.208	-0.350	-0.250	3.940
p value	0.0198	0.0401	0.0710	0.0080	0.3288	0.0018	0.5752	0.8172	0.1364
Sonication time (X6)									
Estimate	-0.251	-0.442	0.115	0.969	0.049	0.592	-1.267	1.725	1.288
p value	0.0346	0.0216	0.3037	0.1595	0.1647	0.0660	0.1080	0.1802	0.5557
Sonication amplitude (X7)									
Estimate	-0.092	-0.573	0.142	1.291	-0.018	0.092	0.150	1.087	-2.140
p value	0.2712	0.0106	0.2246	0.0892	0.5492	0.6903	0.8056	0.3530	0.3523
Drug loading (X8)									
Estimate	0.110	0.880	-0.242	-3.401	-0.089	1.125	11.100	-0.878	4.097
p value	0.2065	0.0031	0.0802	0.0073	0.0434	0.0125	0.0003	0.4408	0.1263

Highlighted cells reflect significant factors to affect the corresponding response.

<sup>a</sup>Q 1 h and Q 12 h are percentage of simvastatin released after 1 and 12 h, respectively.

positive sign of the estimate value illustrates a direct relationship of the variable nominal value with the response, whereas a negative sign illustrates an inverse relationship. The obtained regression analysis data showed that increasing charging agent and sonication parameters resulted in smaller vesicle formation, and both experimental amphiphile and drug loadings had most dominant influences on volume- and number-weighted sized, respectively (Figures 1 and 3). On the other hand, increasing cholesterol loading within the amphiphilic matrix of the lamellae was associated with a non-significant increase in niosomal sizes (Figure 1).

Before size reduction by sonication, hydration of the lipid phase produced niosomal suspensions of large multilamellar vesicles. These vesicles showed large variation in size distribution; since large fraction of niosomal vesicles was more than 7  $\mu\text{m}$  in size with a relatively small fraction (<5% by number) of vesicles below 400 nm. After sonication, vesicular sizes decreased and became more homogenous with polydispersity indices more than 0.6 (data not shown). During the sonication process, large niosomes comminuted then reassembled into smaller sizes; whereas very fine niosomal vesicles might fuse together to result in a more homogenous

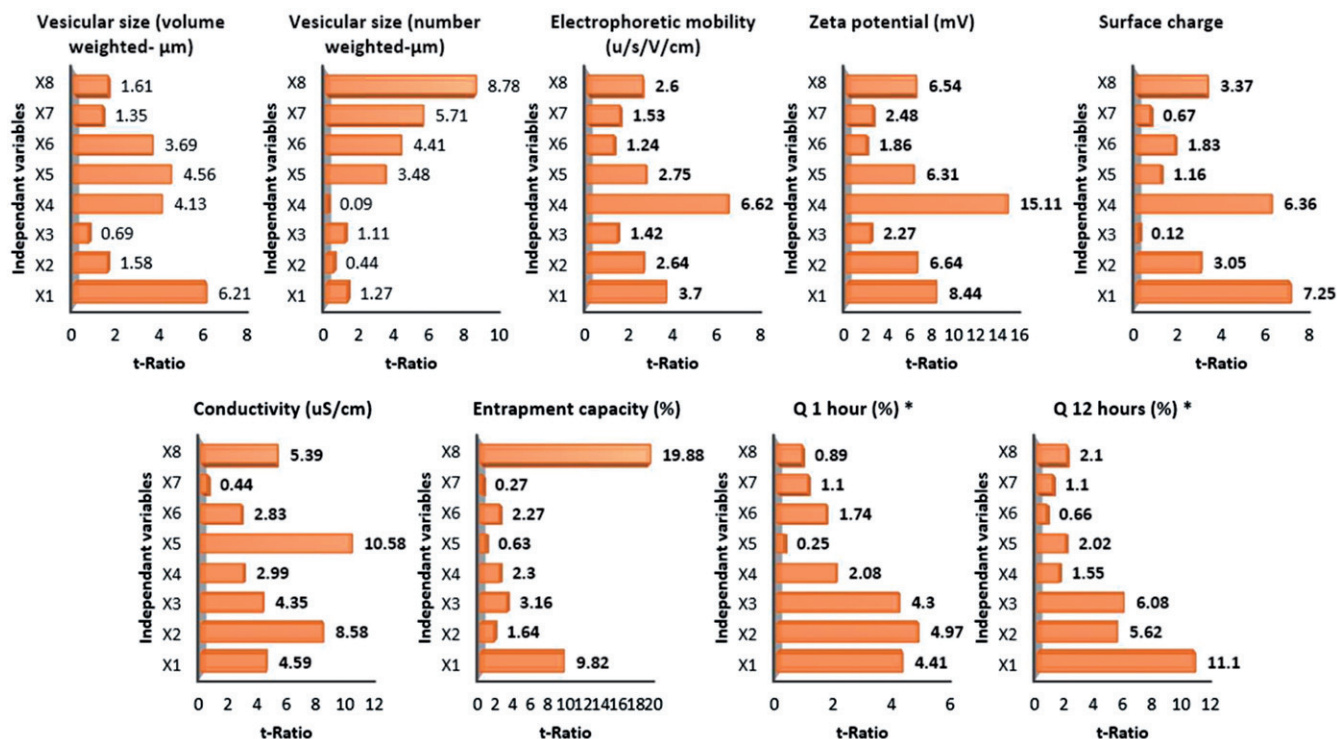


Figure 1. Pareto charts showing the standardized effect of the investigated variables on the studied responses. Q 1 h and Q 12 h are percentage of simvastatin released after 1 and 12 h, respectively. X1–8 are surfactant loading in moles, surfactant chain length, cholesterol loading in moles, charging agent type (negative charge), percentage of charging agent, sonication time in seconds, sonication amplitude and drug loading in moles, respectively. \*-refers to a description for the abbreviations “Q 1h and Q 12h”.

size distribution (Arunothayanun et al., 2000; Liu et al., 2010). Woodbury et al. explained this ultrasound action to comminute large vesicles by a cavitation mechanism, caused by oscillating microbubbles, to produce shear fields (Woodbury et al., 2006). Within these fields, large vesicles tended to form long tube-like appendages that could pinch-off into smaller vesicles. The contribution of the negatively charged dicetyl phosphate to decrease the niosomal sizes during sonication can be explained by the difference in fatty acid chain lengths. Dicetyl phosphate has a shorter chain length of (16 carbons) than that of span 60 (18 carbons) that might interfere with the lamellar packing assembly. Considering the same amount and type of amphiphile molecules were assembled into lamellar structure, this action could result in both a greater curvature of the lamellae to form smaller vesicles and a smaller internal volume to entrap less hydrophilic drug molecules (Fang et al., 2006). Yamaguchi explained also this phenomenon by the high electrical potential of dicetyl phosphate at the niosomal surface that repelled the lamellae to form smaller vesicles owing to electrostatic repulsion (Yamaguchi, 1996; Knudsen et al., 2012). The significant positive effect of both amphiphile and drug loading on the niosomal sizes could be explained by the mass action of entrapping lipophilic drug molecules within the formed lamellar matrix (Alsarra, 2009). To summarize, the formulation and processing variabilities could significantly influence niosomal sizes as well as the integrity of lamellar structure, and successively affected the drug entrapment. Within the investigated design space, it was concluded that a smaller unilamellar niosomes would result in higher simvastatin entrapment capacity (EC).

The predictability of the number-weighted niosomal sizes by the model was acceptable ( $p = 0.0184$ ) with regression coefficients ( $R^2$ ) of 0.9807 for plotting the predicted number-weighted vesicular sizes versus the actual values, respectively (Figure 2). After neglecting the insignificant variables, the reduced linear model equation that explain the effect of only the significant variables on vesicular sizes can be expressed by the following equations. X1–X8 are surfactant loading in moles, surfactant chain length, cholesterol loading in moles, charging agent type (negative charge), percentage of charging agent, sonication time in seconds, sonication amplitude and drug loading in moles, respectively

Volume-weighted vesicular size

$$= 2.8 + 0.42 \times \left[ \frac{[X1 - 1.5]}{0.5} \right] - 0.31 \times \left[ \frac{[X5 - 7.5]}{2.5} \right] - 0.25 \times \left[ \frac{[X6 - 45]}{15} \right],$$

Number-weighted vesicular size

$$= 1.48 - 0.34 \times \left[ \frac{[X5 - 7.5]}{2.5} \right] - 0.44 \times \left[ \frac{[X6 - 45]}{15} \right] - 0.5[X7] + 0.8 \times \left[ \frac{[X8 - 0.4]}{0.2} \right]$$

### Surface's electrical properties

Inducing charges at the vesicular surface alters the niosomal physicochemical characteristics and its interaction with biological membranes, since electrostatic phenomena govern

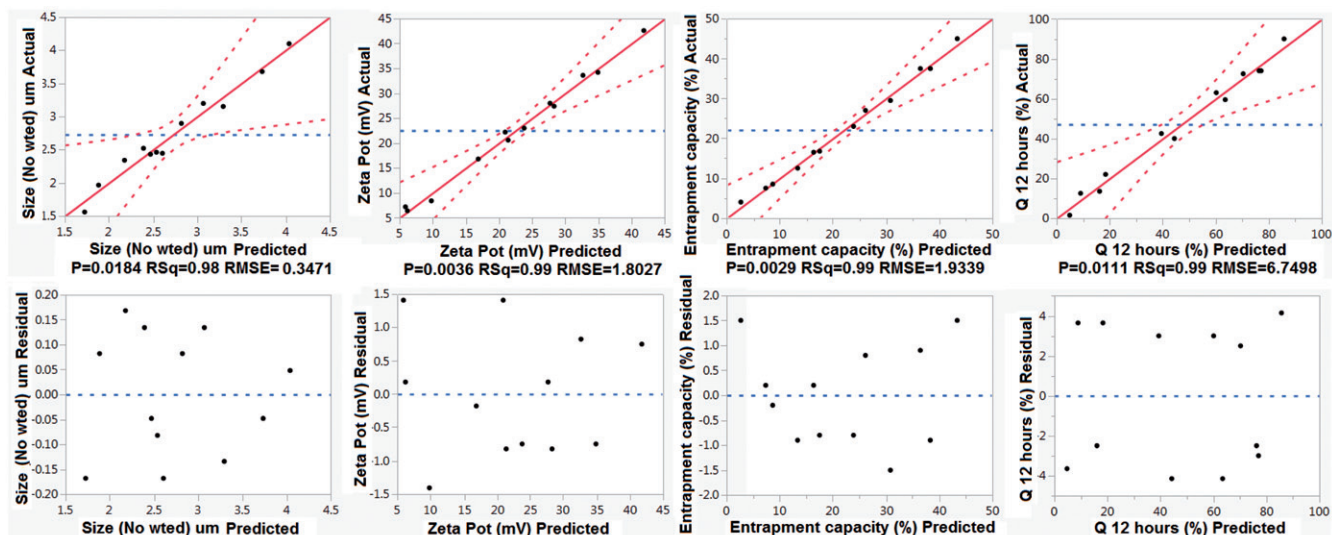


Figure 2. Quantile–quantile and predicted versus the residuals plots for predicting the investigated responses. (Size-No wted is the number-weighted vesicular size; Q 12 h is percentage of simvastatin released after 12 h).

many biological processes. Based on the double layer theory, the analysis of surface charges and electrical double layer around the lipid vesicles by electrophoresis have been performed by many researchers (Franzen & Ostergaard, 2012). The zeta potential could be demarcated as “the electrical potential at the slipping plane that separates the stationary and mobile phases in tangential flow of the liquid with respect to the vesicular surface” (Leroy et al., 2013). Nevertheless, the development of electrokinetics has demonstrated that the determination of zeta potential provides data about the charge beyond the hydrodynamically stagnant layer with minimal description of the mobile counter charges inside of the stagnant layer. However, the extent of the zeta potential can be miscalculated if electrophoretic mobilities are not normalized for the retardation and relaxation forces associated with the electrical conductivity of the vesicles (Revil & Glover, 1997; Lyklema & Minor, 1998). Therefore, the combined determination of conductivity, zeta potential, charge intensity and electrophoretic mobility of the prepared niosomal vesicles would provide better insight about both the stream of matter with charge (electrophoresis) and that of charge without medium flow (Matsumura et al., 2001). For the different factor combinations throughout the 12 formulations, Table 2 shows that the electrophoretic mobilities, zeta potentials and conductivity varied from  $0.5 \mu\text{s}/\text{V}/\text{cm}$  (F6) to  $3.57 \mu\text{s}/\text{V}/\text{cm}$  (F10), from  $6.36 \text{ mV}$  (F6) to  $42.55 \text{ mV}$  (F10) and from  $12 \mu\text{S}/\text{cm}$  (F6) to  $22 \mu\text{S}/\text{cm}$  (F7), respectively. Regarding the net charge type, Table 2 shows that formulations F1, F3, F4, F7, F9, F10 and F12 exhibited negative charges. On the other hand, formulations F2, F5, F6, F8 and F10 were positively charged. The most significant factors affecting the electrophoretic mobilities, zeta potentials and conductivity of the liposomal suspension were amphiphile, charging agent and simvastatin loadings ( $p < 0.05$ ) within the lamellar matrix relative to other variables (Table 3 and Figure 1). On the other hand, cholesterol concentration was only significant for its effect on the vesicular conductivity. The obtained results showed that increasing surfactant, cholesterol and dicetyl phosphate concentrations resulted in

significant increase in the electrical parameters, and dicetyl phosphate concentration had a more prevailing effect (Figures 1 and 3). In addition, increasing fatty acid chain length of the amphiphile was enhancing only the resultant zeta potential and conductivity. On the other hand, increasing experimental simvastatin loading resulted in significant reduction in all electrical parameters.

Increasing the fatty acid chain length and experimental loading of the employed amphiphile caused the zeta potential more negative. Balakrishnan et al. (2009) explained this behavior by increasing the surface free energy of the span surfactants as their tails' volume increase. This behavior could demonstrate that head groups modulate the surface charge in relation to the tail group volume. The higher the tail volume, as in span 60, the higher was the negative charge (Disalvo & Bouchet, 2014). In this case, it would be expected that the higher the negative charge the higher would be the association of the negatively charged dicetyl phosphate molecules at the lamellar surface. Similar observation was observed by Balakrishnan and co-workers where inclusion of the negatively charged lipid, dicetyl phosphate, in the span 20, span 40 and brij 76 niosomes not only decreased the vesicle size but also increased the curvature of the bilayer. This increased the electrostatic repulsion between the ionized head group, thus increasing both the hydrophilic surface area and the resultant zeta potential (Balakrishnan et al., 2009). Contrary to this prediction, the electrical parameters varied to lower negative values with the increase in simvastatin EC (formulation F4, Tables 2 and 3 and Figure 3). The shift to less negative potentials could be ascribed to the orientation of the drug molecules with the acyl groups toward the lamellar surfaces. This observation would strongly suggest that electrostatic charges were not the only driving forces in the entrapment of simvastatin molecules within the amphiphilic matrix. The degree of covering ( $\theta$ ) by dicetyl phosphate molecules can be calculated by relating the zeta potential changes at each dicetyl phosphate loading. The degree of coverage could be expressed as fraction of area, namely  $\alpha_{\text{occupied}}/\alpha_{\text{total}}$ . Moreover, the total amphiphile area could be expressed as

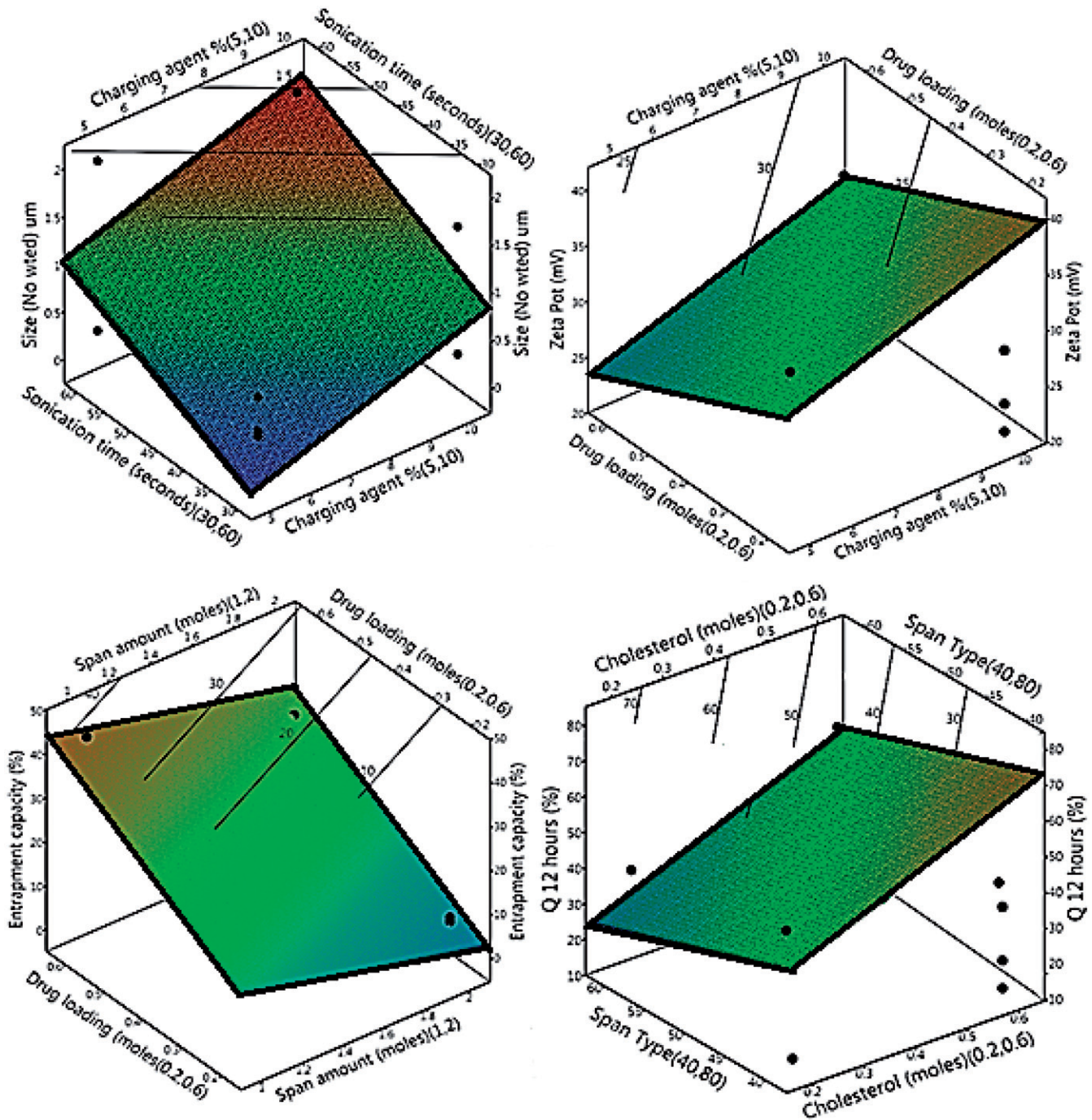


Figure 3. Response surface and contour plots of selected significant factors on the responses. (Size-No wted is the number-weighted vesicular size; Q 12 h is percentage of simvastatin released after 12 h).

$n_L \times a_L$  (where  $n_L$  and  $a_L$  are the number of lipid molecules and the area per molecule, respectively) provided the area per lipid molecule was kept constant at each fatty acid chain length of the surfactant. Hence,  $\theta$  could be calculated from the zeta potential values for each dicetyl phosphate loading according to the following equation (Disalvo & Bouchet, 2014):

$$\theta = \frac{Z_0 - Z}{Z_0 - Z_{\max}}$$

where  $Z_0$  is the recorded zeta potential of niosomal suspension in the absence of dicetyl phosphate,  $Z_{\max}$  is the recorded

zeta potential for niosomal suspension saturated with maximum dicetyl phosphate loading, and  $Z$  is the recorded zeta potential at any medium value of dicetyl phosphate loading. Thus, if  $Z$  equaled  $Z_0$ ,  $\theta$  and the  $\alpha_{\text{occupied}}/\alpha_{\text{total}}$  would be 0. On the other hand, if  $Z$  equaled  $Z_{\max}$ ,  $\theta$  and the  $\alpha_{\text{occupied}}/\alpha_{\text{total}}$  would be 1. From the previous equation, it could be demonstrated that when  $n$  equaled 1, the association stoichiometry would be 1:1 dicetyl phosphate–amphiphile loading. When  $n < 1$ , more dicetyl phosphate association at the surface could be expected. Considering this surface association followed a Langmuir type isotherm ( $n = 1$ ). The adsorption isotherm of dicetyl phosphate on span 60 at 25 °C, for which

$n=0.42$ , suggested that the surface association was site-independent, probably producing surface rearrangements. This deviation of dicetyl phosphate surface association from a Langmuir type could explain the drug adsorption at the niosomal surface, and hence less negative zeta potentials were detected (Table 3 and Figure 3).

The positive influence of neutral cholesterol on the electrophoretic mobilities could be explained by the increase in the hydrodynamically counter charges in the double layer (Matsumura et al., 2001). This behavior could be originated from the shift of hydrodynamic slipping plane toward the niosomal surface. On the other hand, the presence of negative charge on the niosomal vesicles could be suggestive of its kinetic stability due to the London dispersion forces (Casals et al., 2003). Thus, constraints should be applied to the incorporated concentrations of dicetyl phosphate and simvastatin loadings to maintain the required entropy of the surface ion distribution and subsequently produced sufficient repulsive force for the kinetic stability of the niosomal dispersion. The effects of other variables were minimal with confidence  $p$  values approaching the non-significant limit ( $p>0.1$ ); hence, they were neglected to develop the predictability function. The constructed model showed good predictability of  $p=0.0036$  for zeta potential estimation with quantile–quantile correlation coefficients of 0.9923 (Figure 2). The linear reduced model equation to predict the zeta potential of the niosomal dispersion can be expressed as

$$\begin{aligned} \text{Zeta potential (mV)} &= 25.9 + 4.39 \times \left[ \frac{[X1 - 1.5]}{0.5} \right] + 6.9 \times \left[ \frac{[X2 - 60]}{20} \right] \\ &+ 3.2 \times \left[ \frac{[X5 - 7.5]}{2.5} \right] - 3.4 \times \left[ \frac{[X8 - 0.4]}{0.2} \right] \end{aligned}$$

### Simvastatin entrapment

For the various factor combinations, Table 2 shows that the EC varied from 4.1% (F9) to 44.9% (F4). As shown in Table 3 and Figure 1, the most significant variables affecting EC were amphiphile, cholesterol and simvastatin experimental loadings ( $p<0.05$ ) relative to other variables. Regarding the formulation variables, the obtained results showed that decreasing both amphiphile and cholesterol concentrations while increasing theoretical simvastatin loading would contribute to higher EC, and amphiphile concentration had a more predominant influence (Figure 1). Both lamellarity and simvastatin solubility in the hydration media contributed to the resultant EC of niosomal matrix. Speculating that the vesicle's core and lamellae were saturated with aqueous medium, this would result in simvastatin distribution within the vesicular layers. Compared with the initial theoretical drug loading, the entrapment efficiency of simvastatin increased by increasing the theoretical amphiphile concentration. On the other hand, expressed as EC, the moles of simvastatin entrapped per each mole of the employed lipid pool were decreased by increasing the lipid concentration. Mokhtar et al. (2008) described this behavior by the fact that the mole fraction of lipid taking part in encapsulation

decreased as the concentration of amphiphile increased. Alinchenko et al. (2005) applied Monte Carlo simulation models for the entrapment of lipophilic moieties into lipidic vesicles to describe the effect of cholesterol on EC. The authors found that cholesterol loading resulted is not only a reduction of the density of the polar group at the interfacial region of the lamella but also an increase in the packing intensity of the amphiphile tails at the middle of the lamella. In addition, Monte Carlo simulation models proposed by Yau et al. (1998) also suggested that the amphiphile head group and the interface lamellar region were more hydrated in cholesterol-rich membranes than in membranes without cholesterol. Hence, it could be expected that the entrapment of the hydrophobic simvastatin molecules would be higher at lower cholesterol loading. When simvastatin experimental loading was increased from 0.3 moles to 0.9 moles, a positive influence on EC values was observed. EL-Samaligy et al. (2006) clarified this result by the saturation of the hydration media with simvastatin, hence forced drug molecules to be encapsulated into the bilayer hydrophobic phase. Hence, for the optimization study, it is advisable to keep this factor at its higher level to maximize the EC, whereas the formulation allows the entrapment of higher drug dose per unit weight of the niosomal gels.

Regarding the process variability on EC, sonication time and amplitude were non-significant variables with  $p$  values of 0.1081 and 0.8056, respectively, with more contribution by the sonication time (Table 3 and Figure 1). In particular, sonication time was negative for its effect on EC, whereas sonication amplitude was positive. At longer sonication time, a substantial amount of the entrapped drug molecules repartitioned out of the lamellar matrix due to increasing the temperature of the media. It could be assumed that simvastatin leakage occurred at high temperature of longer sonication time as a consequence of the enhanced mobility of surfactant's acyl chains (Magin & Niesman, 1984). On the other hand, the enhanced EC by increasing the sonication amplitude could be attributed not only to the rearrangement of the lipid molecules to increase ratio of lamellar matrix to internal volume, hence allowed for higher drug encapsulation, but also to redistribution the homogenization of simvastatin inside and outside liposomes (Xu et al., 2011). Regarding predictability of the multiple regression model, the prediction confidence level of the model to EC was 91.6% and a good correlation was obtained between the observed and predicted values as indicated by the  $R^2$  value of 0.9923 (Figure 2). After neglecting the insignificant variables, the reduced linear model equation that explains the effect of significant factors on EC can be expressed as

$$\begin{aligned} \text{EC} &= 23 - 5.48 \times \left[ \frac{[X1 - 1.5]}{0.5} \right] - 1.76 \times \left[ \frac{[X3 - 0.4]}{0.2} \right] \\ &+ 11.1 \times \left[ \frac{[X8 - 0.4]}{0.2} \right] \end{aligned}$$

### Simvastatin release

As shown in Figure 4, all the release profiles showed the features of a sustained drug release. Hence, two release points (Q 1 h and Q 12 h: percentages simvastatin released after 1

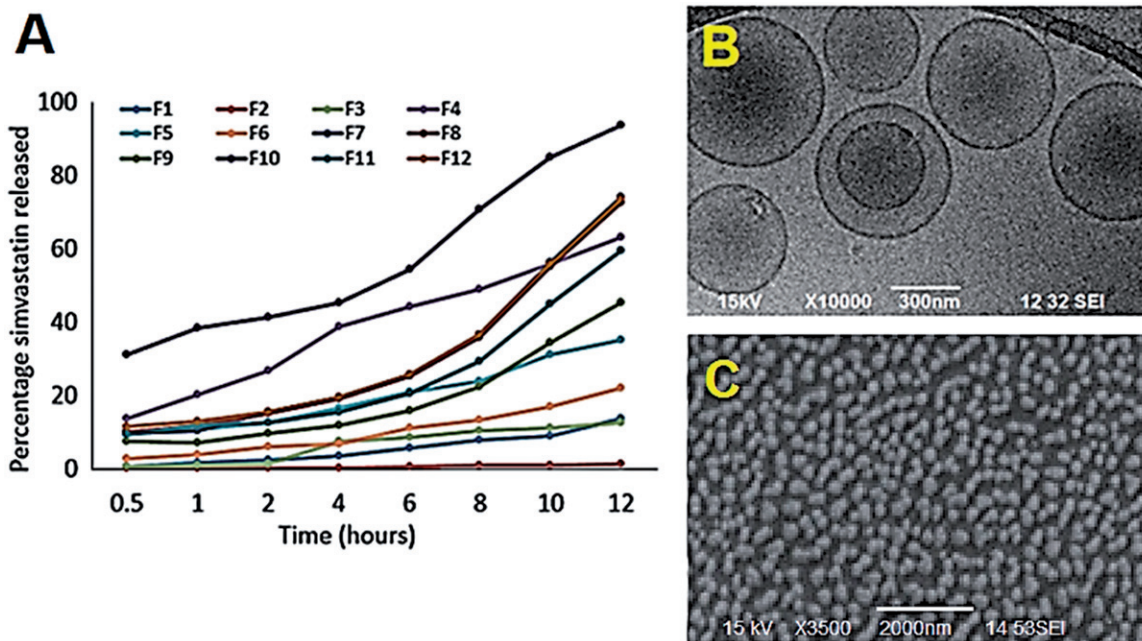


Figure 4. (A) Release profiles of simvastatin from the 12 niosomal formulations using Franz diffusion cells (dialysis membrane MWCO 20 kDa cellulose ester, 10 mM phosphate buffer (pH 6.8) containing 0.05% sodium dodecyl sulfate, 37 °C, 300 rpm,  $n = 3$ ). Standard deviation did not exceed 5% of the release percentage at each time point. (B) and (C) TEM and SEM of the prepared niosomal vesicles of highest simvastatin release (F10), respectively.

and 12 h, respectively) were selected to compare the variables combination in retarding the drug release within 12 h. It is worth noting that after 1 h of drug release, below 15% of simvastatin was detected due to the diffusion of the free drug; except formulations F4 and F10 that released 17% and 32% of the drug, respectively (Table 2). In the current study, the acceptance criterion of the free drug after 1 h was set to be not more than 15%. Moreover, if the free drug percentages exceeded 15% within the first hour, then another purification method rather than the ultracentrifugation would be required to remove excess free drug. It should also be noted that the diffusion of free simvastatin through dialysis membrane was kept at the maximum rate to prevent the dialysis membrane from being limiting step for the drug release. This was achieved using dialysis membrane with MWCO of 20 kDa to have a marginal effect on the drug diffusion rate. Accordingly, the diffusion of simvastatin solution in 0.05% sodium dodecyl sulfate reached 90% in about 2 h, which was the maximum diffusion rate that could be attained.

During the initial stage,  $Q_1$  h and  $Q_{12}$  h were fluctuating from 0.15% (F2) to 32.57% (F10) and from 1.36% (F2) to 89.77% (F10), respectively (Table 2). As shown in Figure 1 and Table 3, compared with other factors, amphiphile chain length, amphiphile and cholesterol concentrations showed significant effects ( $p < 0.05$ ) on both  $Q_1$  h and  $Q_{12}$  h. The obtained results showed that less drug leaked out after 2 and 12 h by increasing both amphiphile concentration and acyl chain length (Figure 3 and Table 3). On the other hand, both release parameters increased by increasing cholesterol loading within the lamellar matrix (Figure 3). Simvastatin release rates from span 60-based niosomes were slower than those from span 20-based formulations. At 25 °C, the long fatty acid

chain of span 60 were in ordered gel state, but those of span 20 were in a disordered liquid-crystalline state to facilitate drug leakage (Das & Palei, 2011). The inclusion of cholesterol within the lamellar structure disrupted the ordered array of the hydrocarbon chains in the gel phase (Alinchenko et al., 2005). Apparently, at higher cholesterol level, the bilayer mobility cannot hold out the osmotic difference to burst release the entrapped and adsorbed drug from the niosomal surface (Liang et al., 2004).

A kinetic analysis of simvastatin release was performed using the Korsmeyer–Peppas model that suitable in situations different release phenomena are involved in spherical systems (Hayashi et al., 2005). The following kinetic equation has been applied to release profiles, where  $K$  is a constant that influenced by the physicochemical properties of the investigated simvastatin-loaded niosomes,  $n$  is the order of drug release to indicate the suggested release mechanism and  $F$  symbolizes the percentage released of simvastatin at time each time point.

$$F = Kt^n$$

If  $n$  values were between 0 and 0.5, the release mechanism would follow the Fickian diffusion transport pathway. On the other hand, if  $n$  values lied between 0.5 and 1, convective mass transfer phenomenon (anomalous transport) would be more prominent (Pando et al., 2013). Fitting the recorded release data according to the Korsmeyer–Peppas model yielded  $n$  values that did not exceed 0.5 to indicate Fickian diffusion models (data not shown). The developed prediction model showed good predictability of  $p = 0.0048$  and  $0.0111$  for  $Q_1$  h and  $Q_{12}$  h with quantile–quantile correlation coefficients of 0.9638 and 0.9855, respectively (Figure 2).

The linear reduced model equations to predict both responses are given below

$$Q1\ h = 15.18 - 4.37 \times \left[ \frac{[X1 - 1.5]}{0.5} \right] - 9.85 \times \left[ \frac{[X2 - 60]}{20} \right] + 4.26 \times \left[ \frac{[X3 - 0.4]}{0.2} \right],$$

$$Q12\ h = 58.03 - 21.63 \times \left[ \frac{[X1 - 1.5]}{0.5} \right] - 21.89 \times \left[ \frac{[X2 - 60]}{20} \right] + 11.83 \times \left[ \frac{[X3 - 0.4]}{0.2} \right]$$

### Analysis of variance

Quantile–quantile plots of regressing the measured niosomal characteristics against the corresponding predicted values yielded linear correlations, where  $R^2$  values were exceeding 0.9 (Figure 2). The mean relative percentage deviations between the predicted and actual values of all responses were not exceeding  $\pm 8\%$ . Plotting the residuals against the corresponding predicted value for each response showed a random scattered pattern about zero; hence, the presence of missing values, non-constant variance or outliers can be excluded. This signposted the validity of analysis of variance (ANOVA) results since the normality of the experimental data distribution was evidenced (Figure 2). In addition, the Cook's distances values for the investigated responses were not close to the corresponding threshold values proposing the absence of outliers or abnormalities. At 95% confidence level of ANOVA and degree of freedom of 8 for all responses, sum of squares of 5.43, 17.39, 8.76, 1432.97, 1.00, 142.14, 1927.62, 849.63 and 9306.18 with mean squares of 0.68, 2.17, 1.10, 179.12, 0.13, 17.77, 240.95, 106.20 and 1163.27 were obtained for volume and number-weighted niosomal sizes, electrophoretic mobility, zeta potential, surface charge, conductivity, EC, Q 1 h and Q 12 h, respectively (Table 4). Values of the root-mean-squared error (RMSE), the  $F$ -ratio, the  $\text{Prob} > F$  value,  $R^2$ , the adjusted correlation coefficient ( $\text{Adj-}R^2$ ) and the lack of fit  $F$ -ratio (FLOF) were used to evaluate the predictability of the constructed models.  $R^2$  values were in good agreement with the corresponding  $\text{Adj-}R^2$  values to indicate good fittings, meaning that at least 95% of variation in the investigated responses could be explained by the fitted models (Figure 2). This was confirmed by the  $F$ -ratios and  $\text{Prob} > F$  values: the formers (12.17, 18.04, 10.58, 55.12, 14.85, 33.97, 64.43, 9.01 and 25.53 for volume and number-weighted niosomal sizes, electrophoretic mobility, zeta potential, surface charge, conductivity, EC, Q 1 h and Q 12 h, respectively) were much greater than their critical values, while the latters were as low as 0.0321, 0.0184, 0.0392, 0.0036, 0.0243, 0.0073, 0.0029, 0.0488 and 0.0111 for volume and number-weighted niosomal sizes, electrophoretic mobility, zeta potential, surface charge, conductivity, EC, Q 1 h and Q 12 h, respectively (Table 4). As also indicated by low RMSE values that were less than 3%, the

Table 4. Summary of ANOVA testing for evaluating the significance of the model in portions.

Responses*	ANOVA parameters				
	DF	SS	MS	$F$ ratio	$\text{Prob} > F$
Vesicular size ( $\mu\text{m}$ )					
Volume weighted	8	5.43	0.68	12.17	0.0321
Number weighted	8	17.39	2.17	18.04	0.0184
Electrophoretic mobility ( $\mu\text{s/V/cm}$ )	8	8.76	1.10	10.58	0.0392
Zeta potential (mV)	8	1432.97	179.12	55.12	0.0036
Surface charge	8	1.00	0.13	14.85	0.0243
Conductivity ( $\mu\text{S/cm}$ )	8	142.14	17.77	33.97	0.0073
EC (%)	8	1927.62	240.95	64.43	0.0029
Release data <sup>a</sup>					
Q 1 h (%)*	8	849.63	106.20	9.01	0.0488
Q 12 h (%)*	8	9306.18	1163.27	25.53	0.0111

<sup>a</sup>Q 1 h and Q 12 h are percentages of the drug released after 1 and 12 h, respectively. \*-refers to a description for the abbreviations ‘‘Q 1h and Q 12h’’.

fitted model and the experimental data were within 95% confidence level. The FLOF values were below the corresponding critical values to emphasize that the lack of fit for all responses were non-significant relative to the pure errors. Hence, the results of the ANOVA models demonstrated the validity of the constructed models to predict the investigated responses within the selected design space.

### Microscopic analysis

The shape and surface characteristics of the prepared niosomes were inspected by TEM and SEM analysis. Figure 4(B) shows the SEM and TEM images of formulation F10 that exhibited 90% Q 12 h and 8.5% EC. The average diameter of the niosomal vesicles was homogeneously distributed and estimated about 300 nm, which was in a good agreement with that obtained by the light scattering technique (number-weighted vesicular size of 0.31  $\mu\text{m}$  (Table 2). Neither aggregation nor vesicular fusions were observed to indicate the efficiency of the sizing technique to maintain the vesicles' integrity. TEM image shows that the niosomes maintained their spherical shape even on simvastatin entrapment.

### *In vivo* hypolipidemic activity

The pharmacodynamic activity of simvastatin concerns with reduction of the elevated cholesterol and TG concentrations in blood. In addition, it elevates HDL concentration in blood to potentiate clearance of cholesterol from peripheral tissues back for hepatic metabolism. This well-established pharmacological activity is described as dose-dependent (van Wijk et al., 2005). Therefore, this pharmacological activity was used to compare the *in vivo* hypolipidemic performance of the prepared transdermal niosomes with the raw oral simvastatin suspension.

TG-rich diet containing 25% soybean oil, 1.0% cholesterol, 13% fiber and 4538.4 kcal/kg was used to induce hyperlipidemia in animals. This diet was successful to elevate cholesterol and TG concentrations in animals' blood at 5, 10 and 15 days. After administering simvastatin to the different assigned groups for five days, the percentages

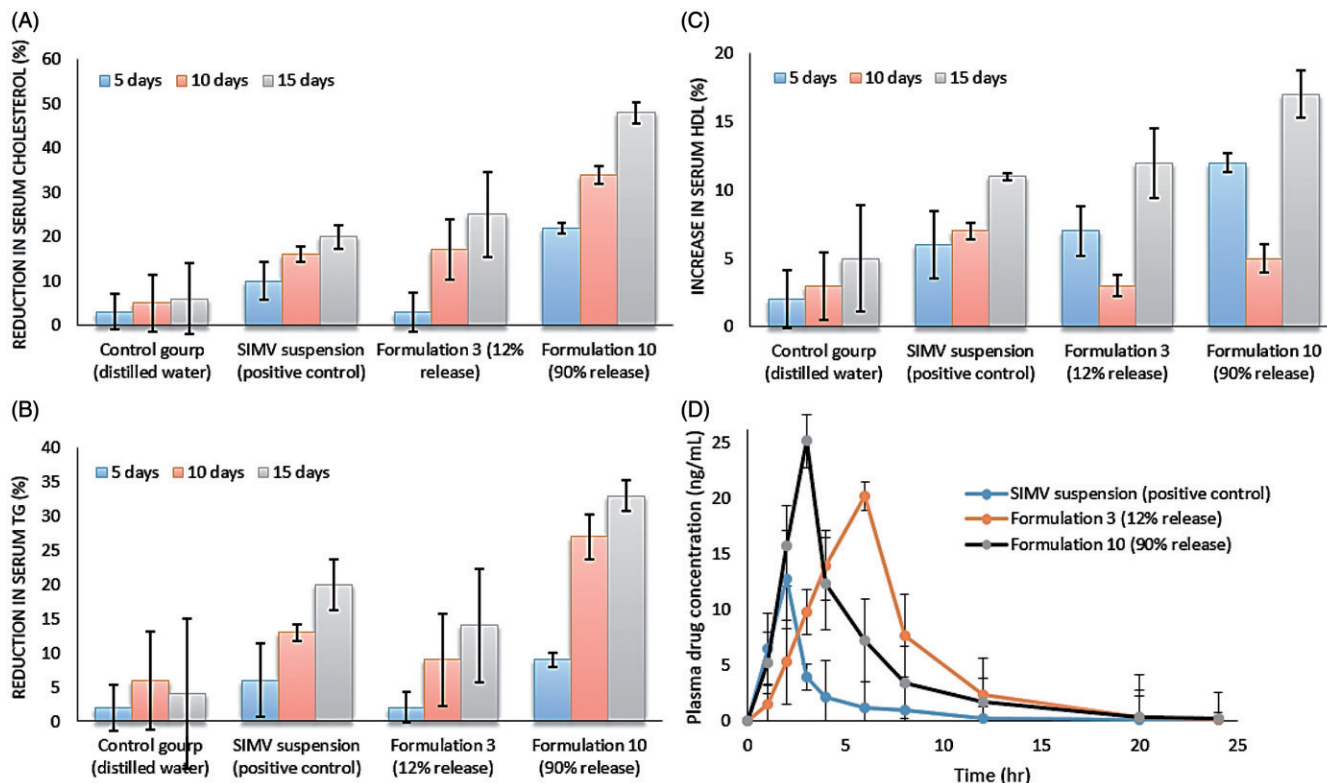


Figure 5. (A), (B) and (C) percent changes in serum cholesterol, TG and HDL levels of experimental groups at different time intervals. (D) Plasma drug concentrations–time profiles of oral simvastatin suspension and its transdermal niosomal formulations of lowest and highest drug release rates (F3 and F10).

reduction in cholesterol concentration were  $3.28 \pm 2.31\%$  and  $22.46 \pm 4.38\%$  for formulations F3- and F10-treated groups, respectively, as compared with oral drug suspension. After 10 and 15 days of administration, formulation F10 reduced cholesterol level significantly ( $34.85 \pm 6.34\%$  and  $48.25 \pm 5.32\%$ , respectively), followed by formulation F3 ( $17.92 \pm 5.31\%$  and  $25.17 \pm 4.25\%$ , respectively) as compared with oral drug suspension ( $15.26 \pm 3.72\%$  and  $20.74 \pm 9.17\%$ , respectively), ( $p < 0.05$ ) (Figure 5A). Regarding protection against hypercholesterolemia, formulation F10 was higher compared with formulation F3 than that of oral drug suspension. The later showed greater intersubject variation ( $SD = 9.1\%$ ) than the transdermal formulations. In the same way, the decline in plasma TG concentrations after transdermal treatment with both niosomal formulations was greater after 5, 10 and 15 days as compared with oral simvastatin suspension. Formulation F10 displayed significant percent reduction in TG concentration ( $33.27 \pm 3.15\%$ ) as compared with oral drug suspension at 15 days of administration ( $p < 0.05$ ) (Figure 5B). When the protection factor, HDL levels, was analyzed and compared, higher concentrations were detected for both niosomal formulations, F3 and F10, as compared with simvastatin suspension. After 15 days of treatment,  $17.73 \pm 4.82\%$  increase in plasma HDL concentration was detected for formulation F10 followed by formulation F3 ( $12.64 \pm 2.98\%$ ) as compared with simvastatin suspension ( $11.57 \pm 7.73\%$ ) (Figure 5C). The significant decline in plasma cholesterol and TG concentrations in addition to the rise in HDL concentration by formulation F10 followed by formulation F3 can be referred to higher drug release rates and permeation through rat skin which in turn

enhanced simvastatin absorption. These findings indicate that proposing simvastatin in a niosomal transdermal formulation was effective to control hyperlipidemia as compared with its raw oral suspension.

### Bioavailability analysis

The plasma concentration–time profiles for simvastatin after both oral dosing of its suspension and transdermal administration of niosomal formulations (F3 and F10) are shown in Figure 5(D). The pharmacokinetic parameters for all groups were calculated using Kinetica software (Kinetica 5.0.11, Thermo Fisher Scientific Inc., Waltham, MA) (Table 5). Formulations F3 and F10 showed simvastatin concentrations in blood compared with its oral suspension. The  $AUC_{total}$  for formulation F10 was found to be  $10.24 \times 10^{-5} \mu\text{g}/\mu\text{L h}$ , which was significantly ( $p < 0.005$ , *one-way ANOVA and Bonferroni's multiple comparison test*) greater than that of oral drug suspension ( $3.52 \times 10^{-5} \mu\text{g}/\mu\text{L h}$ ), while it was non-significant different for formulation F3 ( $11.82 \times 10^{-5} \mu\text{g}/\mu\text{L h}$ ). The same trend was observed for  $AUMC_{total}$  values that were  $18.1 \times 10^{-5}$ ,  $78.2 \times 10^{-5}$  and  $74.3 \times 10^{-5} \mu\text{g}/\mu\text{L h}$  for oral drug suspension, formulations F3 and F10, respectively. When the  $C_{max}$  values were compared, significant augmentation was observed in the case of formulation F10 compared with oral suspension ( $p < 0.0001$ , *one-way ANOVA followed by Bonferroni's multiple comparison test*), while there was no significant difference when compared with formulation F3. This enhanced bioavailability after transdermal administration of both niosomal formulations could be ascribed to a combination of the following factors: first, niosomal vesicles

Table 5. Mean pharmacokinetics parameters<sup>a</sup> of 20 mg/kg simvastatin oral suspension administered to group I (positive control,  $n=6$ ) and 20 mg/kg simvastatin niosomal gel (formulations F3 and F10) transdermal administration to groups II and III (test,  $n=6$ ), respectively.

	Simvastatin suspension (positive control)	Formulation 3 (12% release)	Formulation 10 (90% release)
$C_{max}$ ( $\mu\text{g/L}$ )	12.73	20.23	25.2
$T_{max}$ (h)	2.2	5.84	3.02
$AUC_{total}$ ( $\mu\text{g}/\mu\text{L}\cdot\text{h}$ )	$3.52 \times 10^{-5}$	$11.82 \times 10^{-5}$	$10.24 \times 10^{-5}$
$Kel$ ( $\text{h}^{-1}$ )	0.47	0.24	0.21
$AUMC_{total}$ ( $\mu\text{g}/\mu\text{L}\cdot\text{h}^2$ )	$18.1 \times 10^{-5}$	$78.2 \times 10^{-5}$	$74.3 \times 10^{-5}$
$T_{half}$ (h)	2.74	7.77	7.35
MRT (h)	2.13	6.62	5.31

<sup>a</sup>Standard deviations did not exceed 10% of the stated values.

allowed a delivery vector for simvastatin to cross the skin barriers. Second, niosomal vesicles were introducing simvastatin as a fine dispersion compared with coarse particles in the case of drug suspension, hence an increased surface area with reduced diffusion path length. Third, a higher adhesion surface contact between niosomal vesicles and absorption site was afforded. Fourth, transdermal administration avoided the first-pass hepatic metabolism after oral dosing (Gambhire et al., 2011).

When  $T_{max}$  values after dosing with niosomal formulations was compared, shortest  $T_{max}$  was observed in the case of formulation F10, which could be due to fastest drug release rates. When  $T_{half}$  and MRT of the prepared formulations were compared with those after oral administration,  $T_{half}$  and MRT of formulation F3 ( $7.77 \pm 0.43$  h and  $6.62 \pm 0.52$  h, respectively) were higher followed by formulation F10 ( $7.35 \pm 0.91$  h and  $5.31 \pm 1.21$  h, respectively) and drug suspension ( $2.74 \pm 0.21$  h and  $2.13 \pm 0.33$  h, respectively). This results could be ascribed to slower simvastatin absorption (lipophilic molecule with  $\log P = 4.68$ ) through the stratum corneum, which in turn serves as the drug reservoir for extended release into the viable epidermis over hours (Morgan et al., 1998). The relative bioavailabilities of formulations F3 and F10 were 335.8 and 290.9 with respect to oral drug suspension. Thus, there were 3.35 and 2.9 folds increase in simvastatin bioavailability of the drug from formulations F3 and F10, respectively, by application of its niosomal gel onto the skin.

## Conclusion

Using the Plackett–Burman screening statistical design, niosomal transdermal delivery system of simvastatin was developed for pediatric population and was subjected to *in vitro* and *in vivo* characterization. The formulation and processing variables were classified for their influence on the critical niosomal characteristics. Moreover, *in vivo* pharmacokinetic investigations in rats showed an augmentation in simvastatin bioavailability from its transdermal niosomal formulations by about 3 folds, compared with oral drug suspension. The results were well supported by investigating the corresponding hypolipidemic effects to show a significant enhancement of the biological activities. In conclusion, simvastatin niosomal gels could be considered as promising

transdermal drug delivery system for treatment of hyperlipidemic pediatric patients.

## Declaration of interest

This project was funded by the Deanship of Scientific Research (DSR), King Abdulaziz University, Jeddah, under grant No. (431/166/1434). The authors, therefore, acknowledge with thanks DSR technical and financial support.

## References

- Ah YC, Choi JK, Choi YK, et al. (2010). A novel transdermal patch incorporating meloxicam: *in vitro* and *in vivo* characterization. *Int J Pharm* 385:12–19.
- Alinchenko MG, Voloshin VP, Medvedev NN, et al. (2005). Effect of cholesterol on the properties of phospholipid membranes. 4. Interatomic voids. *J Phys Chem B* 109:16490–502.
- Alsarra IA. (2009). Evaluation of proniosomes as an alternative strategy to optimize piroxicam transdermal delivery. *J Microencapsul* 26: 272–8.
- Amati L, Chiloiro M, Jirillo E, et al. (2007). Early pathogenesis of atherosclerosis: the childhood obesity. *Curr Pharm Des* 13:3696–700.
- Ammar HO, Salama HA, El-Nahhas SA, et al. (2008). Design and evaluation of chitosan films for transdermal delivery of glimepiride. *Curr Drug Deliv* 5:290–8.
- Arunothayanun P, Bernard MS, Craig DQ, et al. (2000). The effect of processing variables on the physical characteristics of non-ionic surfactant vesicles (niosomes) formed from a hexadecyl diglycerol ether. *Int J Pharm* 201:7–14.
- Balakrishnan P, Shanmugam S, Lee WS, et al. (2009). Formulation and *in vitro* assessment of minoxidil niosomes for enhanced skin delivery. *Int J Pharm* 377:1–8.
- Bariya SH, Gohel MC, Mehta TA, et al. (2012). Microneedles: an emerging transdermal drug delivery system. *J Pharm Pharmacol* 64: 11–29.
- Belay B, Belamarich PF, Tom-Revzon C. (2007). The use of statins in pediatrics: knowledge base, limitations, and future directions. *Pediatrics* 119:370–80.
- Browne B, Vasquez S. (2008). Pediatric dyslipidemias: prescription medication efficacy and safety. *J Clin Lipidol* 2:189–201.
- Casals E, Galán AM, Escobar G, et al. (2003). Physical stability of liposomes bearing hemostatic activity. *Chem Phys Lipids* 125:139–46.
- Ceballos LT, Angelín BP, García CR. (2008). Use of statins in children. *An Pediatr* 68:385–92.
- Dahl-Jorgensen K, Larsen JR, Hanssen KF. (2005). Atherosclerosis in childhood and adolescent type 1 diabetes: early disease, early treatment? *Diabetologia* 48:1445–53.
- Daniels SR, Greer FR, Committee on Nutrition. (2008). Lipid screening and cardiovascular health in childhood. *Pediatrics* 122:198–208.
- Das MK, Palei NN. (2011). Sorbitan ester niosomes for topical delivery of rofecoxib. *Indian J Exp Biol* 49:438–45.
- Disalvo EA, Bouchet AM. (2014). Electrophoretic mobility and zeta potential of liposomes due to arginine and polyarginine adsorption. *Colloids Surf A: Physicochem Eng Asp* 440:170–4.
- El-Menshawe SF, Hussein AK. (2013). Formulation and evaluation of meloxicam niosomes as vesicular carriers for enhanced skin delivery. *Pharm Dev Technol* 18:779–86.
- El-Samaligy MS, Afifi NN, Mahmoud EA. (2006). Increasing bioavailability of silymarin using a buccal liposomal delivery system: preparation and experimental design investigation. *Int J Pharm* 308: 140–8.
- El-Say KM, Ahmed TA, Badr-Eldin SM, et al. (2014). Enhanced permeation parameters of optimized nanostructured simvastatin transdermal films: *ex vivo* and *in vivo* evaluation. *Pharm Dev Technol* 2014 Jul 14:1–8. [Epub ahead of print].
- Fang JY, Hwang TL, Huang YL, et al. (2006). Enhancement of the transdermal delivery of catechins by liposomes incorporating anionic surfactants and ethanol. *Int J Pharm* 310:131–8.
- Franzen U, Ostergaard J. (2012). Physico-chemical characterization of liposomes and drug substance-liposome interactions in pharmaceuticals using capillary electrophoresis and electrokinetic chromatography. *J Chromatogr A* 1267:32–44.

- Gambhire M, Bhalekar M, Shrivastava B. (2011). Bioavailability assessment of simvastatin loaded solid lipid nanoparticles after oral administration. *AJPS* 6:251–8.
- Gelissen IC, Nguyen HL, Tiao DK, et al. (2014). Statin use in Australian children: a retrospective audit of four pediatric hospitals. *Paediatr Drugs* 16:417–23.
- Hakanen M, Lagstrom H, Kaitosaari T, et al. (2006). Development of overweight in an atherosclerosis prevention trial starting in early childhood. The STRIP study. *Int J Obes (Lond)* 30:618–26.
- Hayashi T, Kanbe H, Okada M, et al. (2005). Formulation study and drug release mechanism of a new theophylline sustained-release preparation. *Int J Pharm* 304:91–101.
- Jiang T, Han N, Zhao B, et al. (2012). Enhanced dissolution rate and oral bioavailability of simvastatin nanocrystal prepared by sonoprecipitation. *Drug Dev Ind Pharm* 38:1230–9.
- Kang BK, Lee JS, Chon SK, et al. (2004). Development of self-microemulsifying drug delivery systems (SMEDDS) for oral bioavailability enhancement of simvastatin in beagle dogs. *Int J Pharm* 274:65–73.
- Knudsen NO, Ronholt S, Salte RD, et al. (2012). Calcipotriol delivery into the skin with PEGylated liposomes. *Eur J Pharm Biopharm* 81: 532–9.
- Leroy P, Devau N, Revil A, et al. (2013). Influence of surface conductivity on the apparent zeta potential of amorphous silica nanoparticles. *J Colloid Interface Sci* 410:81–93.
- Liang X, Mao G, Ng KY. (2004). Mechanical properties and stability measurement of cholesterol-containing liposome on mica by atomic force microscopy. *J Colloid Interface Sci* 278:53–62.
- Liu B, Mazouchi A, Gradinaru CC. (2010). Trapping single molecules in liposomes: surface interactions and freeze-thaw effects. *J Phys Chem B* 114:15191–8.
- Lyklema J, Minor M. (1998). On surface conduction and its role in electrokinetics. *Colloids Surf A* 140:33–41.
- Magin RL, Niesman MR. (1984). Temperature-dependent permeability of large unilamellar liposomes. *Chem Phys Lipids* 34:245–56.
- Matos SL, Paula HD, Pedrosa ML, et al. (2005). Dietary models for inducing hypercholesterolemia in rats. *Braz Arch Biol Technol* 48: 203–9.
- Matsumura H, Verbich SV, Dimitrova MN. (2001). Surface conductivity of counter ions on protein-adsorbed lipid liposomes. *Colloids Surf A: Physicochem Eng Asp* 192:331–6.
- Mokhtar M, Sammour OA, Hammad MA, et al. (2008). Effect of some formulation parameters on flurbiprofen encapsulation and release rates of niosomes prepared from proniosomes. *Int J Pharm* 361: 104–11.
- Morgan TM, Reed BL, Finin BC. (1998). Enhanced skin permeation of sex hormones with novel topical spray vehicles. *J Pharm Sci* 87: 1213–18.
- Newman III WP, Freedman DS, Voors AW, et al. (1986). Relation of serum lipoprotein levels and systolic blood pressure to early atherosclerosis. The Bogalusa Heart Study. *N Engl J Med* 314:138–44.
- Pando D, Gutiérrez G, Coca J, et al. (2013). Preparation and characterization of niosomes containing resveratrol. *J Food Eng* 117:227–34.
- Pandya P, Gattani S, Jain P, et al. (2008). Co-solvent evaporation method for enhancement of solubility and dissolution rate of poorly aqueous soluble drug simvastatin: in vitro-in vivo evaluation. *AAPS PharmSciTech* 9:1247–52.
- Patty PJ, Frisken BJ. (2006). Direct determination of the number-weighted mean radius and polydispersity from dynamic light-scattering data. *Appl Opt* 45:2209–16.
- Pesonen E. (1989). Preliminary and early stages of atherosclerosis in childhood. *Zentralbl Allg Pathol* 135:545–8.
- Revil A, Glover PWJ. (1997). Theory of ionic-surface electrical conduction in porous media. *Phys Rev B* 55:1757–73.
- Schwab KO, Doerfer J, Krebs A, et al. (2007). Early atherosclerosis in childhood type 1 diabetes: role of raised systolic blood pressure in the absence of dyslipidaemia. *Eur J Pediatr* 166:541–8.
- Sibley C, Stone NJ. (2006). Familial hypercholesterolemia: a challenge of diagnosis and therapy. *Cleve Clin J Med* 73:57–64.
- Smith DG. (2007). Epidemiology of dyslipidemia and economic burden on the healthcare system. *Am J Manag Care* 13:S68–71.
- Tavano L, Alfano P, Muzzalupo R, et al. (2011). Niosomes vs microemulsions: new carriers for topical delivery of Capsaicin. *Colloids Surf B Biointerfaces* 87:333–9.
- Tiwari R, Pathak K. (2011). Statins therapy: a review on conventional and novel formulation approaches. *J Pharm Pharmacol* 63:983–98.
- van Wijk JP, Buirma R, van Tol A, et al. (2005). Effects of increasing doses of simvastatin on fasting lipoprotein subfractions, and the effect of high-dose simvastatin on postprandial chylomicron remnant clearance in normotriglyceridemic patients with premature coronary sclerosis. *Atherosclerosis* 178:147–55.
- Varshosaz J, Tavakoli N, Salamat FA. (2011). Enhanced dissolution rate of simvastatin using spherical crystallization technique. *Pharm Dev Technol* 16:529–35.
- Who-Report. (2012). Country cooperation strategy for WHO and Saudi Arabia 2006–2011 [Online]. Available from: [http://www.who.int/countryfocus/cooperation\\_strategy/ccs\\_sau\\_en.pdf](http://www.who.int/countryfocus/cooperation_strategy/ccs_sau_en.pdf) [last accessed 20 May 2013].
- Woodbury DJ, Richardson ES, Grigg AW, et al. (2006). Reducing liposome size with ultrasound: bimodal size distributions. *J Liposome Res* 16:57–80.
- Xu X, Khan MA, Burgess DJ. (2011). A quality by design (QbD) case study on liposomes containing hydrophilic API: I. Formulation, processing design and risk assessment. *Int J Pharm* 419:52–9.
- Xu X, Khan MA, Burgess DJ. (2012). A quality by design (QbD) case study on liposomes containing hydrophilic API: II. Screening of critical variables, and establishment of design space at laboratory scale. *Int J Pharm* 423:543–53.
- Yamaguchi T. (1996). Lipid microspheres as drug carriers: a pharmaceutical point of view. *Adv Drug Deliv Rev* 20:117–30.
- Yau WM, Wimley WC, Gawrisch K, et al. (1998). The preference of tryptophan for membrane interfaces. *Biochemistry* 37:14713–18.
- Zidan AS, Mokhtar M. (2011). Multivariate optimization of formulation variables influencing flurbiprofen proniosomes characteristics. *J Pharm Sci* 100:2212–21.
- Zidan AS, Rahman Z, Khan MA. (2011). Product and process understanding of a novel pediatric anti-HIV tenofovir niosomes with a high-pressure homogenizer. *Eur J Pharm Sci* 44:93–102.